

## Effects of induced currents on *Dst* and on magnetic variations at midlatitude stations

Lasse V. T. Häkkinen, Tuija I. Pulkkinen, Heikki Nevanlinna,  
Risto J. Pirjola, and Eija I. Tanskanen  
Finnish Meteorological Institute, Helsinki, Finland

Received 10 October 2000; revised 17 August 2001; accepted 17 August 2001; published 24 January 2002

[1] Magnetic variations observed at Earth's surface are primarily caused by magnetospheric and ionospheric currents and secondarily affected by currents induced within Earth. For studies of space processes it is necessary to separate the internal contribution from the external one. In this paper we consider the *Dst* index which reflects the properties of the ring current. A spherical harmonic analysis is applied, using the axisymmetric assumption, to make the separation of magnetic data to external and internal parts. By examining 12 storms in 1997 and 1998, our results show that during the storm main phase the internal contribution to *Dst* is roughly 30%, after which it decreases to about 20% during the recovery phase. This is supported by an approximate model calculation of the induction in Earth. We also consider *H* variations at the four *Dst* observatories (Honolulu, San Juan, Hermanus, Kakioka) separately and at a typical continent station (Boulder) for comparison. It is seen that Kakioka systematically has the largest internal contribution during the storm main phase, while Hermanus has only a very small internal part at that time. The three other stations are closer to the ideal case (i.e., the internal part is roughly 1/3). As the anomalous behavior at Kakioka is thus opposite to that at Hermanus, their effects approximately average out in the computation of *Dst*. The differences between the stations are obviously due to differences in local ground conductivity structures. This conclusion is supported by investigating the Parkinson induction vectors which are larger at Kakioka and Hermanus than at the other observatories. **INDEX TERMS:** 2778 Magnetospheric Physics: Ring current, 1515 Geomagnetism and Paleomagnetism: Geomagnetic induction, 2788 Magnetospheric Physics: Storms and substorms

### 1. Introduction

[2] The *Dst* index, computed as the average depression of the horizontal magnetic field component at four low-latitude stations, gives a measure of the effect of the external current systems on the low-latitude geomagnetic field [Mayaud, 1980; Rangarajan, 1989]. Traditionally, the *Dst* index has been interpreted to reflect variations in the intensity of the symmetric part of the ring current encircling Earth at altitudes ranging from 3 to 8  $R_E$ . Approximately, the relation between the ring current intensity and depression at the center of Earth can be given in the form of the Dessler-Parker-Sckopke formula [Dessler and Parker, 1959; Sckopke, 1966]:

$$\frac{\Delta B}{B_0} = \frac{2W}{3W_m}, \quad (1)$$

where  $\Delta B$  is the field decrease due to the ring current,  $B_0$  is the average equatorial surface geomagnetic field,  $W = \int wdV$  is the total energy of the ring current particles or the energy density integrated over the ring current volume, and  $W_m \sim 10^{18}$  J is the energy in Earth's dipole field above the surface. However, if (when) the plasma density is nonzero at the outer edge of the ring current, this formula can be given in a more accurate (and complex) form including these effects [Tverskoy, 1997]. Several studies that have estimated the ring current from in situ magnetospheric particle

measurements have concluded that the field depression computed from the particle energy is significantly smaller than that predicted by the Dessler-Parker-Sckopke (DPS) formula [e.g., Hamilton *et al.*, 1988; Turner *et al.*, 2001]. On the other hand, Greenspan and Hamilton [2000] found a relatively good agreement of the DPS formula if the quiet time ring current is not subtracted from the measurements.

[3] As any magnetic field measurement, the *Dst* index does not separate between source currents but gives an integral over all existing current systems. The *Dst* index can be corrected for effects of magnetopause currents, which are known to contribute a positive factor to the index. Hence, the so-called pressure-corrected *Dst* index can be computed from

$$Dst^* = Dst - b\sqrt{P_{dyn}} + c, \quad (2)$$

where  $b = 7.26 \text{ nT}/\sqrt{\text{nPa}}$ , the solar wind dynamic pressure  $P_{dyn}$  is given in nanopascals, and  $c = 11$  nT is an estimate for the quiet time ring current and magnetopause current [O'Brien and McPherron, 2000]. Recently, effects of the cross-tail current on *Dst* variations have also been considered: While Alexeev *et al.* [1996] suggest that the tail currents contribute more than half of the *Dst* index, Turner *et al.* [2000] conclude that the cross-tail current contribution to *Dst* is about 25%. However, these estimates also depend on the duration of the disturbance: As an hourly index, *Dst* smooths many variations associated with magnetospheric substorms. It is also important to note that the *Dst* index gives an estimate only of the symmetric part of the ring current. During a storm maximum the ring current is often asymmetric and achieves full symmetry only late in the recovery phase.

[4] A further complication to the interpretation of the *Dst* index comes from the fact that the magnetospheric and ionospheric currents induce currents inside Earth. For magnetospheric research it is important to understand how much of the measured variations actually arise from the current systems external to Earth and how much is due to induction effects that depend on the details of Earth's conductivity structure and its possible local inhomogeneities [Viljanen *et al.*, 1995]. In an idealized situation it can be shown that the internal contribution to  $X$  is half of the external variation, being thus one third of the measured total variation [see Price, 1967, p. 286]. Such a large value underlines the importance of evaluating the induction effects in the magnetic indices such as *Dst*.

[5] The *Dst* index is widely used in various studies of the solar wind–magnetosphere coupling, especially during geomagnetic storms, when a significant portion of the enhanced solar wind energy input is dissipated in the inner magnetosphere ring current region [e.g., Lu *et al.*, 1998]. Several studies utilizing linear and nonlinear filtering techniques have demonstrated a high degree of predictability of the *Dst* index using present and past values of the solar wind, interplanetary magnetic field, and the *Dst* index itself [Lundstedt, 1997; Vassiliadis *et al.*, 1999; O'Brien and McPherron, 2000]. These methods are being further developed to provide reliable estimators of near-future geomagnetic activity conditions for space weather purposes.

[6] Because of the importance of the ring current to storm dynamics and because direct energetic particle observations from the ring current are not always available, the *Dst* index will remain a key element in the analysis of magnetically disturbed periods. Detailed analyses of individual storm events often utilize higher-resolution indices such as symmetric (*SYM*) and asymmetric indices (*ASY*) which are computed using many more than the standard four stations. For both of these indices,  $H$  and  $D$  variations are computed separately, and the *Dst* index is essentially the same as the hourly average of *SYM-H*. While these indices give a better spatial and temporal picture of the time evolution of the system, they are susceptible also to the effects of short-duration non-ring-current-associated current systems. For these reasons it is very important to understand all sources that produce variations to the used index.

[7] In this paper we are only examining one portion of the disturbances measured at midlatitudes, those that represent the symmetric part of the measured current system. Therefore we have also restricted our analysis to a spherically symmetric case, both in considering the external current system as well as Earth's conductivity structure. Furthermore, Earth is modeled by a perfectly conducting sphere below a nonconducting surface layer, as a more detailed structure would bring substantial complications in the computations with limited improvements in accuracy, considering the other approximations made.

[8] The effects of the induced currents depend on Earth's conductivity structure, on the temporal and spatial structure of magnetospheric-ionospheric source currents, and on the location of the measurement point relative to the source current [e.g., Marschall, 1986; Tanskanen *et al.*, 2001]. While horizontal variations in the conductivity structure are difficult to account for, many studies have used either uniformly conducting or layered Earth models including conductivity variations in the vertical direction [e.g., Price, 1967]. Recent developments in modeling lateral variations of Earth's conductivity [Tarits and Grammatica, 2000] would also permit a more complex analysis; however, as stated above, assuming that Earth is one-dimensional is consistent with the axisymmetry associated with the *Dst* index. The largest induction effects are caused by current systems that vary rapidly with time and hence are assumed to be associated with the storm main phase.

[9] In this paper we examine the induction effects on the *Dst* index determined using the four standard *Dst* stations. In section 2 we shortly review the definition and computation of the *Dst* index.

In section 3 we separate the internal and external parts of the *Dst* index using a spherical harmonic expansion. In section 4 we discuss the effects contributing to the internal component of the *Dst* index, and section 5 concludes with a discussion.

## 2. Derivation of *Dst*

[10] *Dst* is an hourly index published since 1957 [Sugiura and Kamei, 1991]. It is calculated from the horizontal  $H$  component at four observatories: Honolulu (dipole latitude and longitude 21.0°N, 266.4°), San Juan (29.9°N, 3.2°), Hermanus (33.3°S, 80.3°) and Kakioka (26.0°N, 206.0°). These observatories were chosen because they lie far enough from both the auroral and the equatorial electrojets and give an even distribution in longitude (see Figure 1).

[11] In this paper we apply the official method for deriving the *Dst* index [see, e.g., Sugiura and Kamei, 1991] to determine the disturbance fields at individual stations and to compute the final *Dst* index. The method consists of two steps. In the first step the secular variation is subtracted from the recorded data, and in the second step the solar quiet daily variation,  $S_q$ , is eliminated. In deriving the *Dst* index, only the  $H$  component of each observatory is used. However, here we apply a similar algorithm also to the  $Z$  components.

[12] The baseline of  $H$  to be subtracted from the data from all four observatories has to account for the secular variation. The baseline is calculated by first determining the annual mean values of  $H$  from the 5 quietest days of each month for the year under consideration and for 4 preceding years. A second-order polynomial fit is then made to the annual mean values to obtain the baseline for each day. The  $H$  data to be used for determining the *Dst* index is then the difference  $\Delta H$  between the observed  $H$  values and the baseline.

[13] To subtract the solar quiet daily variation,  $S_q$ , from the  $\Delta H$  data, we need to know the  $S_q$  curves for each individual day. The official method employs a statistical analysis where  $S_q$  is expanded as a double Fourier series in local time  $T$  and month number  $M$

$$S_q(T, M) = \sum_{m=1}^6 \sum_{n=1}^6 A_{mn} \cos(mT + \alpha_m) \cos(nM + \beta_n). \quad (3)$$

The series consists of 48 unknown coefficients  $A_{mn}$ ,  $\alpha_m$ , and  $\beta_n$ . These are determined by computing one  $S_q$  curve for each month as an average of the variation curves over the 5 quietest days of the month. A possible linear trend from a local midnight to the following local midnight in these  $S_q$  variations is subtracted. These  $S_q$  curves give us 288 data points, so the coefficients may be determined by usual least squares fitting methods. Once the coefficients are known, the  $S_q$  variation may be computed for any day and any hour of the year.

[14] The disturbance variation is then obtained from  $D(T) = \Delta H(T) - S_q(T)$  at any time  $T$ . If we assume that the disturbance causing  $D(T)$  is a symmetric ring current flowing in the magnetic equatorial plane (far from Earth), it causes a magnetic variation only in the direction parallel to the dipole axis. In this case the variation can be obtained from the measurement of the horizontal field by dividing it by  $\cos \lambda$ , where  $\lambda$  is the dipole latitude of the observatory. The *Dst* index is then defined as an average of these variations over the globe,

$$Dst(T) = \frac{1}{4} \sum_{n=1}^4 \frac{D_n(T)}{\cos \lambda_n}. \quad (4)$$

[15] Note that Sugiura and Kamei [1991] give a somewhat different formulation of the *Dst*, in which the horizontal distur-



**Figure 1.** Distribution of *Dst* observatories. The solid line marks the magnetic dip equator [From *Sugiura and Kamei*, 1991].

bances are averaged separately, and the average is divided by the average of the cosines of the latitudes,

$$Dst(T) = \frac{\sum_{n=1}^4 D_n(T)}{\sum_{n=1}^4 \cos \lambda_n}. \quad (5)$$

Using the four stations given here, the differences in the results are not very large. Furthermore, the formulation given by (4) allows us to intercompare the variations measured at each station.

### 3. Separation of the Internal and External Parts of *Dst*

[16] In the region between Earth's surface and the ionosphere, there are no currents, and because the temporal variations are slow, the displacement currents are negligible. The magnetic field is curl-free and can thus be expressed as a gradient of a scalar potential.

[17] Let  $\Delta U$  be a magnetic scalar potential associated with a magnetic field variation caused by current systems external to Earth,  $\Delta \mathbf{B}$ , so that  $\Delta \mathbf{B} = -\nabla \Delta U$ . Because the magnetic field is always divergence-free, the potential satisfies the Laplace equation. The potential can then be divided into an external part  $\Delta U_e$  caused by the external current distribution and an internal part  $\Delta U_i$  corresponding to currents induced inside Earth such that

$$\Delta U = \Delta U_i + \Delta U_e. \quad (6)$$

As solutions of the Laplace equation, these potentials can be expressed as power expansions:

$$\Delta U_i = a \sum_{n=1}^N \left\{ \left( \frac{a}{r} \right)^{n+1} \sum_{m=0}^n [g_{ni}^m \cos(m\phi) + h_{ni}^m \sin(m\phi)] P_n^m(\cos\theta) \right\} \quad (7)$$

$$\Delta U_e = a \sum_{n=1}^N \left\{ \left( \frac{r}{a} \right)^n \sum_{m=0}^n [g_{ne}^m \cos(m\phi) + h_{ne}^m \sin(m\phi)] P_n^m(\cos\theta) \right\}, \quad (8)$$

where  $\theta$  is the dipole colatitude,  $\phi$  is the dipole longitude,  $P_n^m(\cos\theta)$  is the associated Legendre function, and  $a$  is the radius of Earth. The components of the magnetic field can then be derived from the potentials as  $X = (1/r) \partial \Delta U / \partial \theta$ ,  $Y = -(1/(r \sin\theta)) \partial \Delta U / \partial \phi$  and  $Z = \partial \Delta U / \partial r$ .

[18] Because Earth is small in comparison with the size of the ring current radius, we only consider here the first term  $n = 1$  and restrict our analysis to the axisymmetric case ( $m = 0$  and  $Y = 0$ ). Then the internal field components are given by

$$\Delta X_i = -\left( \frac{a}{r} \right)^3 g_{1i}^0 \sin \theta \quad (9)$$

$$\Delta Z_i = -2 \left( \frac{a}{r} \right)^3 g_{1i}^0 \cos \theta. \quad (10)$$

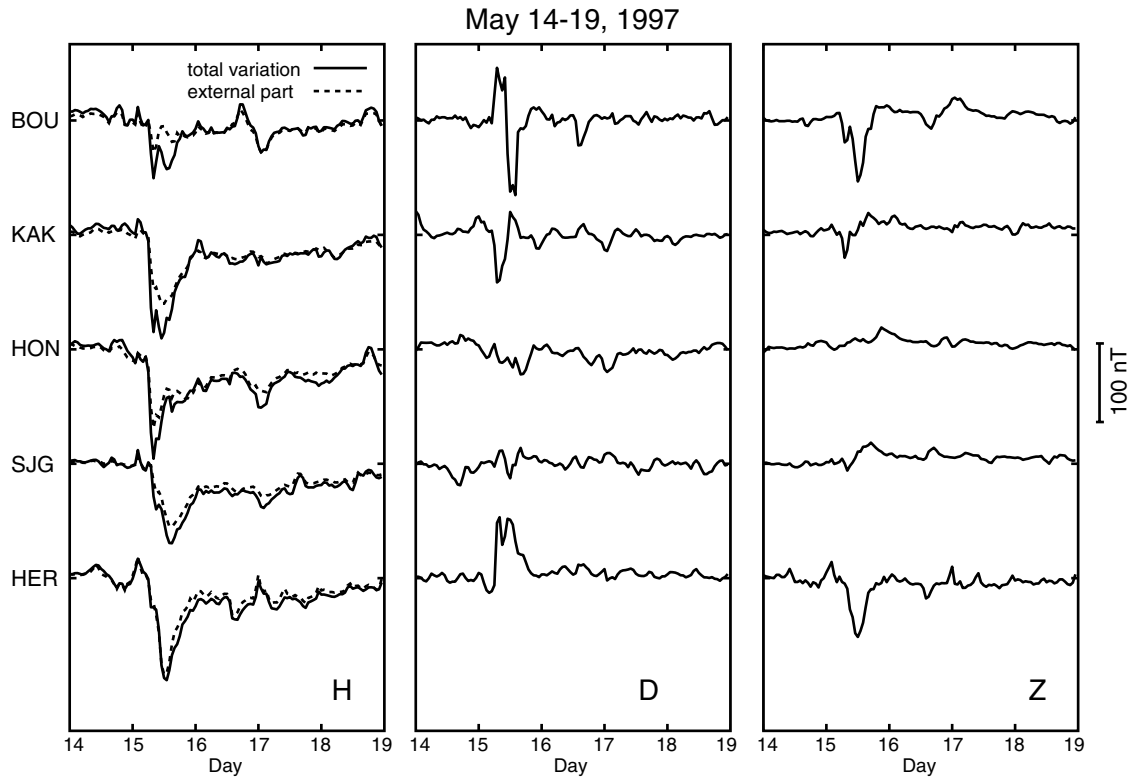


**Figure 2.** Variations of all three magnetic field components ( $H$ ,  $D$ , and  $Z$ ) at the four standard  $Dst$  stations and at Boulder during the magnetic storm on 14–19 May 1997. The dashed lines in the  $H$  component plot show the computed external parts of the field. Differences (in hours) between local time and universal time for different stations are  $-7$  for Boulder (BOU),  $+9$  for Kakioka (KAK),  $-11$  for Honolulu (HON),  $-4$  for San Juan (SJG), and  $+1$  for Hermanus (HER).

These correspond to a field created by a dipole aligned with Earth's dipole axis. The external components are given by

$$\Delta X_e = -g_{1e}^0 \sin \theta \quad (11)$$

$$\Delta Z_e = -g_{1e}^0 \cos \theta. \quad (12)$$

These correspond to a constant external field parallel to the magnetic dipole axis. This is the field arising from a circular current loop ( $R \gg a$ ) near the center of the loop. Physically, this approximation means that we assume that the magnetic variations arise from a ring current approximated by a circular current loop in the dipole equatorial plane and that the internal field caused by the induced currents is a dipole field.

[19] Equations (9)–(12) can be solved for  $g_{1i}^0$  and  $g_{1e}^0$ :

$$g_{1i}^0 = -\frac{1}{3} \left[ \frac{\Delta X}{\sin \theta} + \frac{\Delta Z}{\cos \theta} \right] \quad (13)$$

$$g_{1e}^0 = \frac{1}{3} \left[ -2 \frac{\Delta X}{\sin \theta} + \frac{\Delta Z}{\cos \theta} \right]. \quad (14)$$

Here  $\Delta X = \Delta X_e + \Delta X_i$  and  $\Delta Z = \Delta Z_e + \Delta Z_i$ . We can now write the relation of the external field to the total field strength in the symmetric case at Earth's surface as a function of the (observed) total field strength:

$$\frac{\Delta X_e}{\Delta X} = \frac{g_{1e}^0}{g_{1e}^0 + g_{1i}^0} = \frac{2\Delta X - \Delta Z \tan \theta}{3\Delta X}. \quad (15)$$

Thus this formulation allows us to determine the external part of the field variation at each station separately, after which we can compute the “external  $Dst$ ” using the formulation in section 2.

[20] The definition (equation (5)) is motivated by the interpretation that the majority of the  $Dst$  index arises from a ring current at the magnetic equator. Then it is also implicitly assumed that the magnetic field measured at the  $Dst$  stations would not contain any internal contribution. In this case the measured magnetic field would only have a component parallel to the magnetic dipole axis.

[21] If Earth is considered a conducting sphere with a spherically symmetric conductivity distribution, and if the time variation of the field is fast enough to make the sphere approximately equivalent to a perfect conductor, the  $Z$  component of the field is zero at Earth's surface. This means that currents induced inside Earth create a magnetic field whose vertical component cancels that of the external field. This is due to the fact that any time-dependent magnetic field vanishes within a perfect conductor, and because the normal component of the magnetic field is always continuous, the  $Z$  component measured at the surface also has to be zero. The formula given by Price [1967, p. 286] leads to  $\Delta X_e = 2 \Delta X_i$  when  $n = 1$ . Therefore the total  $\Delta X$  component is 50% larger than the external one, which is consistent with (15) with  $\Delta Z = 0$ . Consequently, in the idealized situation the internal contribution makes the  $Dst$  index 50% larger than the pure ring current contribution would give.

#### 4. Application to Storm Events

[22] In this section we examine several storm events and separate the measured magnetic field variations into external and internal contributions using the formulation above. As the axisymmetry assumption gives  $Y = 0$ , the magnitudes of the  $Y(D)$  variations can be used to give an idea of the accuracy of the approximation. In this same approximation  $H = X$ .

[23] Figure 2 shows a medium-size storm that occurred on 15 May 1997. The magnetic field variations of all three components

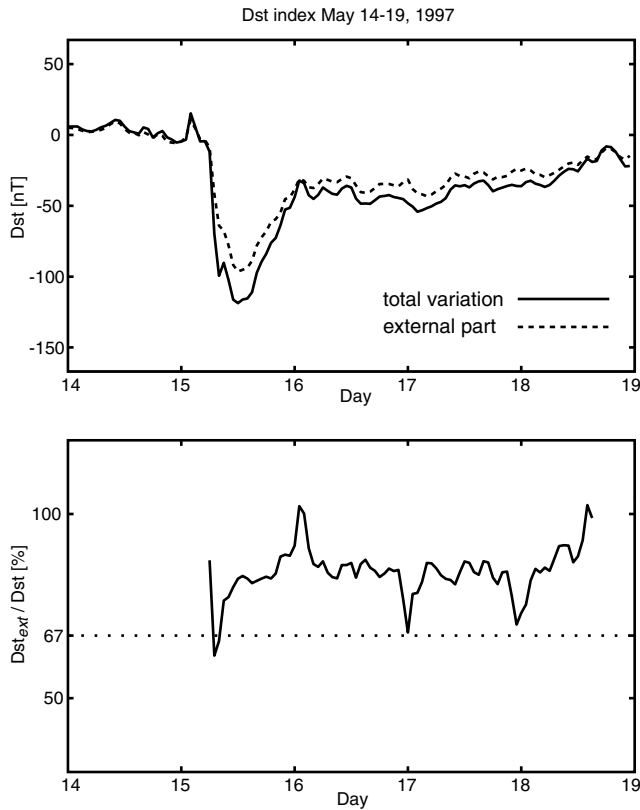


**Figure 3.** (top) *Dst* index as computed from measured field variations (solid line) and as determined by using the external components only (dashed line). (bottom) Ratio of the external *Dst* to the total *Dst*.

(*H*, *D*, and *Z*, all in nanoTesla) are given at the four standard *Dst* stations and at Boulder for reference. Boulder was chosen because it is in the middle of a large continent and thus free from seawater effects. Note that the *D* components were quite large during the main phase of the storm, and that the behavior of *D* varied from station to station: At Boulder, a bipolar spike was seen, with first a positive and then a negative variation. At Kakioka, west of Boulder, there was only a negative variation. Honolulu, in the middle of these stations, records little *D* perturbation, as does San Juan farther east. The most eastward station, Hermanus, again records a strong positive variation. These variations are roughly consistent with a partial ring current flowing out from the ionosphere in the early morning sector and into the ionosphere on the dayside. The *Z* components, which are a measure of the local high-conductivity approximation, were small except for Hermanus and Boulder, where they were large and negative.

[24] The dashed lines in the *H* component plot show the external part of the field separated using (15). Note how the external-to-total field variation varies from station to station: For Boulder and Kakioka, the external components are substantially

**Table 1.** Storm Events in 1997 and 1998

Date, 1997	min <i>Dst</i> , nT	Date, 1998	min <i>Dst</i> , nT
Jan. 10	-78	Feb. 17	-103
April 11	-82	May 4	-216
April 21	-107	June 26	-111
May 15	-115	Aug. 6	-165
Sept. 3	-98	Sept. 18	-76
Oct. 11	-130		
Nov. 7	-110		

smaller than the total measured field, whereas for Hermanus the two curves are nearly identical for the storm main phase, after which there is an almost constant shift in the two curves.

[25] Figure 3 shows the *Dst* index computed from (4) using the measured field variations (solid line) and using the external components only (dashed line). The bottom panel shows the ratio of the external *Dst* to the total measured *Dst* in percent. Note that the ratio reaches the ideal value of 2/3 only during the main phase of the storm; during the storm recovery phase the ratio is typically close to 80%, with a few excursions to lower values that occurred coincident with small enhancements of *Dst*.

[26] In order to study the behavior of the external components more systematically, we examined 12 storms during 1997 and 1998. The storms and their peak (measured) *Dst* values are given in Table 1.

[27] Figure 4 shows results from a superposed epoch analysis for these events. Two times were identified for each storm, the storm onset (positive peak in *Dst* before the main phase, *T*<sub>0</sub>) and the storm main phase maximum (minimum of *Dst*, *T*<sub>1</sub>). Time was then scaled for each of the events so that these two times coincided. The solid lines show the average horizontal variation fields at each

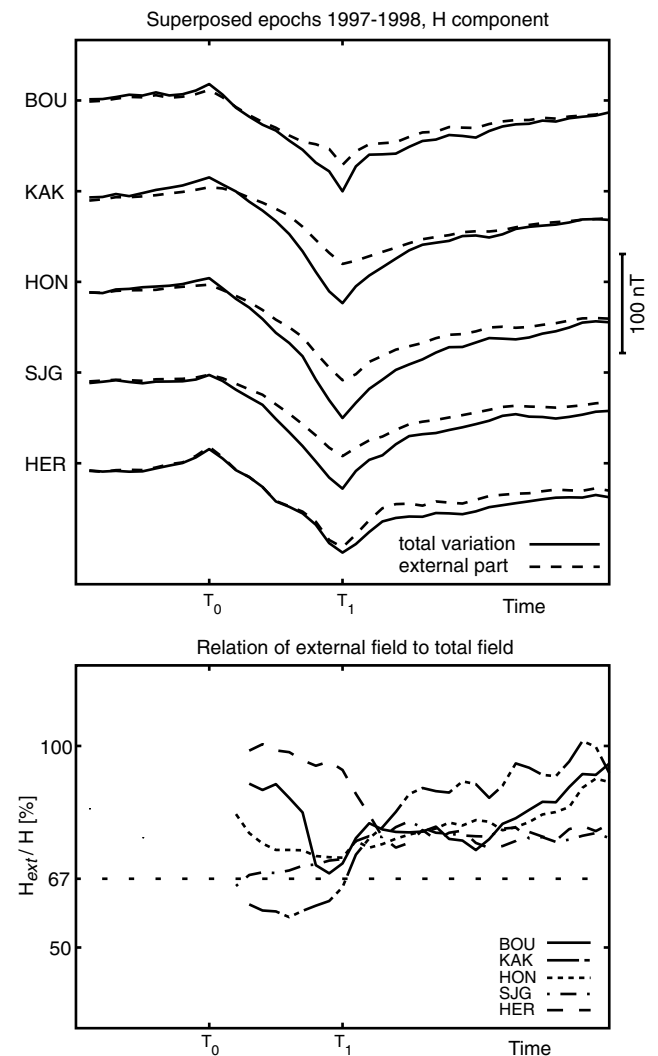


**Figure 4.** Superposed epoch analysis for 12 storm events during 1997 and 1998. (top) the average horizontal variation fields (solid lines) and average external variations (dashed lines) as functions of scaled time. (bottom) The ratios of external field to total field (in percent) for each station separately.

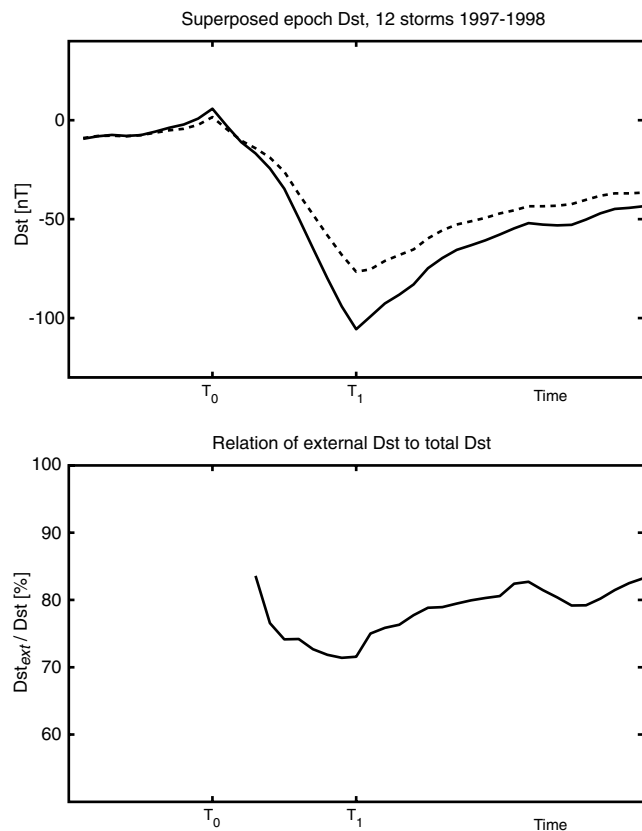


**Figure 5.** Superposed epoch analysis of the *Dst* index. (top) The superposed *Dst* index as determined from measured *H* component variations (solid line) and as computed by using the external field variations only (dashed line). (bottom) Ratio of the external *Dst* to the total *Dst*.

station for these events as a function of the scaled time, where the unit time is the main phase duration.

[28] Similar to Figure 2, the separation of external and internal contributions was made for each storm separately, and the average external variations are shown with the dashed lines. Note how similar the results are to the 15 May 1997 storm event: The external variations are much smaller for Kakioka, whereas Hermanus shows almost no internal contribution during the storm main phase. Because the storm onsets were at very different local times, this behavior is thus independent of the relative locations of the measuring stations to the partial ring current or other strongly contributing currents other than the symmetric ring current. We can therefore conclude that the differences must be caused by structures internal to Earth, which affect the inductive components, and not by spatial structures in the external current systems. The details of Earth's conductivity structure are left for a future study.

[29] The bottom panel of Figure 4 shows the ratios of the external field to the total field for each station separately, again averaged over the set of events. While all curves show variability mostly between 60% and 90%, two curves behave quite differently: Hermanus shows very large values of the ratio (almost no internal component) during the main phase, and reduces then to the smallest values of all stations during the recovery phase. On the other hand, Kakioka measures a large internal contribution during the main phase, and during the recovery phase the ratio shown in Figure 4 exceeds the typical values. Figure 5 summarizes the effects for the *Dst* index computed from the standard stations (excluding Boulder): The internal component is largest and about

30% during the storm main phase and early recovery phase, during the slower recovery the internal field contribution reduces to about 20% of the total field.

[30] The ideal situation, in which the ratio of the external part of *Dst* to the total *Dst* value equals 2/3, requires that Earth can be approximated by a perfectly conducting sphere. As indicated in section 3, this is only acceptable for very rapid time variations (i.e., for characteristic periods of only on the order of seconds). In a much more appropriate model, Earth consists of a perfectly conducting sphere (radius  $b$ ) below a nonconducting surface layer. At  $r = b$ , i.e., at the surface of the perfect conductor, the normal component of the magnetic field  $\Delta Z$  vanishes. Thus using the first terms of the spherical harmonic series expansions (equations (10) and (12)), we obtain

$$g_{1e}^0 = 2\left(\frac{a}{b}\right)^3 g_{1i}^0. \quad (16)$$

Equations (9) and (11) now give the ratio of the external part of  $\Delta X$  (and *Dst*) to the total  $\Delta X$  (and *Dst*) at Earth's surface ( $r = a$ ):

$$\frac{\Delta X_e}{\Delta X} = \frac{2}{2 + \left(\frac{b}{a}\right)^3}. \quad (17)$$

[31] A reasonable value of  $b$  depends on Earth's real conductivity structure [see, e.g., Stacey, 1977, p. 232; Jones, 1982] and on the periods considered. Characteristic periods of the storm main phase and of the recovery phase are roughly 1 hour and 10 hours, respectively. The resistivity ( $\rho$ ) of Earth above the asthenosphere, which lies at a depth of about 200 km, is typically larger than 100  $\Omega$  m. On the basis of the values of the skin depth ( $= \sqrt{T\rho/\pi\mu_0}$ ) the field thus easily penetrates into the asthenosphere during both the main and the recovery phase. As the resistivity of the asthenosphere is only about 1...10  $\Omega$  m, it efficiently attenuates fields having periods around 1 hour, and so a proper value of  $a-b$  during the main phase is 200 km. Periods of 10 hours penetrate through the asthenosphere into the mantle and are strongly attenuated in the highly conducting layers ( $\rho \approx 1$   $\Omega$  m) below 500 km. Hence a suitable value of  $a-b$  during the recovery phase is 600 km.

[32] Substituting the selected values of  $b$  into (17) results in 69% and 73% for the ratio of the external *Dst* to the total *Dst* during the main phase and the recovery phase, respectively. These theoretical estimates approximately agree with our observations based on the data and shown in the bottom panel of Figure 5.

## 5. Discussion and Conclusions

[33] In this paper we have estimated the effects of currents induced in Earth on the *Dst* index using a spherical harmonic expansion of the disturbance field. Our results show that during the storm main phase the internal contribution is about 30%, close to the value obtained for an ideally conducting Earth and perfectly symmetric ring current. On the other hand, during the storm recovery phase the internal contribution is only 20%. This difference obviously reflects the inductive effects arising from rapid variations in the external field that are strongest during the main phase. In this paper the contributions during the main and recovery phase are interpreted in terms of a simple Earth conductivity model containing a perfectly conducting sphere at a given depth.

[34] Because the results were quite similar from event to event, we conclude that these results are independent of the effects caused by asymmetries in the ring current or by varying locations of the *Dst* stations relative to the external current systems. This fact also justifies the assumptions of spherical symmetry of the external current system.

[35] On the other hand, when the field separations were examined for each station separately, it was found that the responses at the various stations were quite different, in a manner that was

consistent from event to event: Kakioka was found to have the largest internal contribution during the storm main phase but smaller than average internal contribution during the storm recovery. The opposite effect, almost no internal contribution during the main phase but larger than average during the recovery phase, was found for Hermanus. The other stations exhibited behavior closer to the ideal case (i.e., a 2/3 external contribution) and were quite similar to each other (including Boulder). It is interesting to note that the anomalous behaviors at Kakioka and Hermanus average out when the *Dst* is computed, and thus the final *Dst* index again behaves closer to the ideal situation during the main phase.

[36] The systematic differences between the stations are most likely caused by differences in the local ground conductivity structure: Kakioka is located at the coast of a highly conducting ocean, which probably increases the induced current contribution there. On the other hand, the Hermanus station is located between the ocean and a large mountainous area with associated deep conductive or resistive structures which probably cause a complicated induction process. At Hermanus, large *Z* component variations are systematically observed during strong *H* variations. Boulder is the only station considered in the middle of a large continent, although the deep structures associated to the high mountains immediately west of the station may affect the measurements as well.

[37] To get a closer understanding about the induction contribution to magnetic variations, we calculated the Parkinson vectors for different events [Parkinson, 1962]. These vectors describe a linear relation between *X*, *Y* and *Z* variations. As the ring current produces a laterally uniform external field locally at the stations, the vectors point toward areas with a high ground conductivity, and the higher the conductivity the larger the magnitude of the vector. Theoretically, the Parkinson vectors should be considered in the frequency domain [e.g., Everett and Hyndman, 1967]. We, however, made a simpler time domain calculation, which resulted in differences between vectors for different events. Anyway, it was seen that the vectors are clearly larger for Kakioka and Hermanus than for Honolulu and San Juan, supporting the above conclusions about complicated induction effects at Kakioka and Hermanus. Boulder also has quite large Parkinson vectors which systematically tend to point toward the mountains. The vectors at Hermanus mostly have directions toward the ocean, indicating the well-known coast effect [Parkinson, 1962] while the three other stations show a larger variety in the directions.

[38] Estimation of the effect of the ground conductivity distribution on the internal component is a nontrivial task, and the outcome strongly depends on the position of the station relative to the current system. Tanskanen et al. [2001] evaluated the internal contribution to the *X* component assuming a finite laterally uniform Earth conductivity for auroral electrojet currents at 100-km altitude. They found that the relative magnitude of the internal contribution varies such that immediately below the electrojet currents the internal contribution is smallest and about 30% of the variation, but farther away the internal contribution increases to 50–60%. These numbers depend on the value of the ground conductivity used. Note that the results were obtained for a layered Earth model, and adding a spatial inhomogeneity increases the complexity of the system. The conclusion that can be drawn from the study by Tanskanen et al. [2001] is that the dependence of the internal contribution on the ground conductivity structure is strongly dependent on geometry, and without further examination, rule-of-thumb estimations cannot be given. This evaluation is left as a future study.

[39] Langel and Estes [1985] used Magsat satellite data for investigating the external and internal contributions to magnetic variations. Similar to this work, their studies were based on spherical harmonic analyses. They concluded that for the axisymmetric parts the ratio between the internal and external contributions to *X* variations is between 0.24 and 0.29 depending on the

time of the day. This means that the internal contribution to measured *Dst* values varies from 19.5 to 22.5%, being thus typically 21%.

[40] The conductivity structure of the real Earth is far from one-dimensional. However, considering a radial conductivity distribution is in agreement with the axisymmetry associated with the *Dst* index. Lateral variations of Earth's conductivity are particularly significant at boundaries between continental and oceanic areas. In a recent paper, Tarits and Grammatica [2000] apply a three-dimensional spherical Earth model in which superficial conductivity heterogeneities describing oceans and continents overlie a one-dimensional medium.

[41] For the use of the *Dst* index in Sun-Earth connection studies it can be concluded from the present work that the internal contribution is about 1/3 for the storm main phase and about 20% during other times including storm recovery. These observations are in agreement with the conclusions by Langel and Estes [1985]. Our results were obtained using hourly averaged data. Using higher time resolution data will emphasize the role of localized, strong current systems that appear especially during substorm activity. Thus higher-resolution data are probably more affected also by the currents induced in Earth than the hourly averages. Furthermore, it is important to notice that while the above result holds for the *Dst* index as well as for data from some of the stations, there are large differences between the individual stations which should be considered separately if their data are used to quantitatively estimate the ring current intensity [e.g., Pulkkinen et al., 2001].

[42] **Acknowledgments.** We wish to thank the INTERMAGNET organization for supplying the magnetometer data. Our thanks also go to Ari Viljanen (FMI) for instructive discussions. We are also grateful to the two referees of the manuscript for their useful and constructive remarks. Particularly significant were the comments and advice about Earth's conductivity models given by one referee.

[43] Michel Blanc thanks Michel Menvielle and another referee for their assistance in evaluating this paper.

## References

- Alexeev, I. I., E. S. Belenkaya, V. V. Kalegaev, Y. I. Feldstein, and A. Grafe, Magnetic storms and magnetotail currents, *J. Geophys. Res.*, **101**, 7737, 1996.
- Dessler, A. J., and E. N. Parker, Hydromagnetic theory of geomagnetic storms, *J. Geophys. Res.*, **64**, 2239, 1959.
- Everett, J. E., and R. D. Hyndman, Geomagnetic variations and electrical conductivity structure in south-western Australia, *Phys. Earth Planet. Inter.*, **1**, 24, 1967.
- Greenspan, M. E., and D. C. Hamilton, A test of the Dessler-Parker-Sckopke relation during magnetic storms, *J. Geophys. Res.*, **105**, 5419, 2000.
- Hamilton, D. C., G. Gloeckler, and F. M. Ipavich, Ring current development during the great geomagnetic storm of February 1986, *J. Geophys. Res.*, **93**, 14,343, 1988.
- Jones, A. G., On the electrical crust-mantle structure in Fennoscandia: No Moho, and the asthenosphere revealed?, *Geophys. J. R. Astron. Soc.*, **68**, 371, 1982.
- Langel, R. A., and R. H. Estes, Large-scale, near-field magnetic fields from external sources and the corresponding induced internal field, *J. Geophys. Res.*, **90**, 2487, 1985.
- Lu, G., et al., Global energy deposition during the January 1997 magnetic cloud event, *J. Geophys. Res.*, **103**, 11,685, 1998.
- Lundstedt, H., AI techniques in geomagnetic storm forecasting, in *Magnetic Storms*, *Geophys. Monogr. Ser.*, vol. 98, edited by B. T. Tsurutani et al., p. 243, AGU, Washington, D. C., 1997.
- Mareschal, M., Modelling of natural sources of magnetospheric origin in the interpretation of regional induction studies: A review, *Surv. Geophys.*, **8**, 261, 1986.
- Mayaud, P. N., *Derivation, Meaning, and Use of Geomagnetic Indices*, *Geophys. Monogr. Ser.*, vol. 22, AGU, Washington, D. C., 1980.
- O'Brien, P., and R. L. McPherron, An empirical phase space analysis of ring current dynamics: Solar wind control of injection and decay, *J. Geophys. Res.*, **105**, 7707, 2000.

- Parkinson, W. D., The influence of continents and oceans on geomagnetic variations, *Geophys. J. R. Astron. Soc.*, **6**, 441, 1962.
- Price, A. T., Electromagnetic induction within the Earth, in *Physics of Geomagnetic Phenomena*, vol. I, edited by S. Matsushita and W. H. Campbell, p. 235, Academic, San Diego, Calif., 1967.
- Pulkkinen, T. I., N. Y. Ganushkina, D. N. Baker, N. E. Turner, J. F. Fennell, J. Roeder, T. A. Fritz, M. Grande, B. Kellett, and G. Kettmann, Ring current ion composition during solar minimum and rising solar activity: POLAR/CAMMICE/MICS results, *J. Geophys. Res.*, **106**, 19,131, 2001.
- Rangarajan, G. K., Indices of Geomagnetic Activity, in *Geomagnetism*, vol. 3, edited by J. A. Jacobs, p. 323, Academic, San Diego, Calif., 1989.
- Sckopke, N., A general relation between the energy of trapped particles and the disturbance field over the Earth, *J. Geophys. Res.*, **71**, 3125, 1966.
- Stacey, F. D., *Physics of the Earth*, 2nd ed., 414 pp., John Wiley, New York, 1977.
- Sugiura, M., and T. Kamei, Equatorial Dst index 1957–1986, in *IGAG Bull. 40*, edited by A. Berthelier, and M. Menvielle, Int. Serv. of Geomagn. Indices Publ. Off., Saint Maur, France, 1991.
- Tanskanen, E. I., A. T. Viljanen, T. I. Pulkkinen, R. J. Pirjola, L. V. T. Häkkinen, A. A. Pulkkinen, and O. Amm, At substorm onset, 40% of AL comes from underground, *J. Geophys. Res.*, **106**, 13,119, 2001.
- Tarits, P., and N. Grammatica, Electromagnetic induction effects by the solar quiet magnetic field at satellite altitude, *Geophys. Res. Lett.*, **27**, 4009, 2000.
- Turner, N. E., D. N. Baker, T. I. Pulkkinen, and R. L. McPherron, Evaluation of the tail current contribution to *Dst*, *J. Geophys. Res.*, **105**, 5431, 2000.
- Turner, N. E., D. N. Baker, T. I. Pulkkinen, J. L. Roeder, J. F. Fennell, and V. K. Jordanova, Energy content in the storm time ring current, *J. Geophys. Res.*, **106**, 19,149, 2001.
- Tverskoy, B. A., Formation mechanism for storm-time ring current structure, *Geomagn. Aeron.*, **37**, 29, 1997.
- Vassiliadis, D., A. J. Klimas, and D. N. Baker, Models of *Dst* geomagnetic activity and of its coupling to solar wind parameters, *Phys. Chem. Earth*, **24**, 107, 1999.
- Viljanen, A., K. Kauristic, and K. Pajunpää, On induction effects at EISCAT and IMAGE magnetometer stations, *Geophys. J. Int.*, **121**, 893, 1995.
- 
- L. V. T. Häkkinen, H. Nevanlinna, R. J. Pirjola, T. I. Pulkkinen, and E. I. Tanskanen, Finnish Meteorological Institute, Geophysical Research, P.O. Box 503, FIN-00101 Helsinki, Finland. (Lasse.Hakkinen@fmi.fi; Heikki.Nevanlinna@fmi.fi; Risto.Pirjola@fmi.fi; Tuija.Pulkkinen@fmi.fi; Eija.Tanskanen@fmi.fi)